2022

Damage in circular flange-bolted connections on behaviour of tall towers, modelled by multilevel substructuring

Prepared by:
Eng. Kosar Raheed Hama

Damage in circular flange-bolted connections on behaviour of tall towers, modelled by multilevel substructuring

Prepared by Eng. Kosar Rasheed Hama

A B S T R A C T

The paper deals with non-linear analysis of a telecommunication tower with circular flange-bolted connections (CFBCs). They are composed of two flanges, welded to the structural tubes, and then connected together with pre-tensioned bolts. A rigorous FEM analysis is performed for finding the connection stiff-ness in two cases. One deals with all bolts undamaged and the second one with one or more bolts broken. The analysis, which includes contact and friction forces, shows that when joints are under tension, the bolts are not only subjected to axial forces, but also to bending moments due the prying effect. The value of stresses caused by bending depends strongly on the bolt pre-tension and flange thickness. Removing one of the six connection bolts significantly increases stresses in the remaining bolts. Knowing the beha-viour of the connection, it is possible to study the behaviour of the whole structure. This is achieved by applying the multilevel substructuring approach. The first levels is related to the flanges and bolts, whereby the connection model is simplified, and compared with the rigorous one, the second level is related to the assembly of the whole tower. The paper is illustrated with several examples of connections of different thicknesses, and different bolt pre-tensions. The considered tower comes from a real design.

1. Introduction

Bolted connections have been used widely for several decades, in many fields of engineering design. Most often, they are applied in the beam-to-column connections. Recently, extensive studies have been devoted to their behaviour, taking into account both sta-tic and dynamic states [1–4].

Joints with bolts have also often been used in the form of flange connections, of different shapes. Circular flange-bolted connections (CFBC) are applied in pressure pipe systems and aircraft engines [5]. In civil engineering structures, CFBCs are mostly used in all kinds of tubular structures.

Circular tubes are widely applied in many structures, such as telecommunication towers, guyed masts and windmills. Usually, these are structures of very large dimensions, which have to be divided in sections owing to assembly constraints. Each section is fabricated (welded) separately, and then, on site all sections are connected together, applying the CFBCs. This is the reason why relatively a lot of attention has been paid to the mechanical behaviour of CFBC and their impact on whole structure response. Cao and Bell [6] discussed widely, among others, the prying effect occurring in these types of joints. Schaumann and Seidel [7] and Schaumann and Kleineidam [8] presented FE modelling and failure analysis of CFBC. Recently, Pavlovic et al. [9] proposed a new design of assembling joints, applying a single overlapping friction connection with long opened slotted hole. The flexural rigidity of bolts and its influence on the behaviour of steel joints has been shown by Abidelah et al. [10].

In engineering design, tubular connections are usually assumed to be pinned or rigid. It was shown by Gutkowski [11] that, such an assumption can lead to significant errors in structural response. Moreover, recent investigations of bolted circular joints showed their complex, non-linear nature, arising mostly from contact forces, friction and bolt pre-stressing. Research in the field over the past two decades deals with several important problems, mostly connection rigidity and its influence on the dynamic behaviour of the total structure. Investigations cover design models, numerical studies, as well as experimental approaches.

Swiercz et al. [12] applied Virtual Distortion Method for identification of bolted joint characteristics in frame structures. In another paper, Blachowski et al. [13] presented a method to localize damage in a frame structure with one loosened bolted

connection. Bogacz et al. [14] investigated bolt connections in railway engineering. Stocki et al. [15] discussed the reliability problem of spot weld joints important for most of automotive industry structures.

The behaviour of the bolted flange connections under monotonic and cyclic loadings is discussed in [16]. The connections were subjected to axial tension forces applied monotonically, for low-cycle and high-cycle fatigue tests. The tests allowed the characterization of the behaviour of connections for this type of loading.

CFBCs play an important role in aircraft engines. Schwingshackl et al. [5] found that the flange model depends strongly on the steady stress/load distribution across the joint and on non-linear elements.

Luan et al. [17] found, by static mechanical investigation, that the axial stiffness of the bolted flange joint is different in tension and compression.

Heinisuo et al. [1] applied the component method for the structural modelling of steel joints in three dimensions. The results of investigation are presented in terms of local and global analysis. The proposed method is verified, for a beam-to-column joint, by a detailed 3D non-linear finite element analysis. Validation of the results is performed with experiments on the end-plate splice joints of rectangular tubular structures.

Couchaux et al. [18] discussed the global behaviour of CFBCs, subjected to complex loadings of bending moment and axial forces. Elastic and elastic–plastic states of the flange material were taken into account.

An important group of papers deals with CFBC defects. Yang et al. [19] proposed the application of a reduced-order modelling technique in damage detection. Numerical results were supported with interesting experiments performed on a shaking table of a 1:3-scale six-storey steel frame structure. The damages of joints are simulated by loosening the connection bolts. Another approach for location of damage in structural connections was presented by Pnevmatikos [20]. He applied Discrete Wavelet Transform to detect plastic hinges within a frame structure subjected to earthquake excitation.

He et al. [21] discussed a lightning mast composed of two pipes, connected together with a bolted flange connection. They proposed applying the global vibration approach, in which models of damaged and undamaged are compared. By introducing a logistic function transformation an unconstrained problem was obtained, which allowed the damage and its magnitude to be localized. The theoretical considerations were in a good agreement with experiments.

Perttola et al. [22] investigated the flanged joint of tubular members experimentally. The joint was subjected to different relative positions of the bending moment and bolts. The test data were compared with a mechanical 3D model.

Hanson et al. [23] evaluated practical, hand formulae for the design of bolted joints in launch vehicles. The formulae, which are based on idealized models, were compared with numerical results, obtained using FEM. Applying the flange model it is possible to observe the non-linear behaviour of a joint under external forces and temperature change.

Patrakkos and Tizani [24] investigated the behaviour of a new kind of anchored blind-bolt connection for concrete-filled hollow profiles. Experimental results showed the forms of the damaged connection through pull-out testing. Degree of dispersion based approach to investigate damage and the loss of stiffness in laboratory-scale beam with flexible connections was presented in the paper by An et al. [25].

All of the above works, theoretical and experimental, show that the mechanical properties of joints are crucial in the design of structures. Among these are CFBCs, which play an important role in the behaviour of the whole structure, in both static and dynamic cases.

In the present paper, a rigorous FEM analysis of CFBCs, applied in tubular towers, is presented. The analysis contains such effects as, contact and friction, together with pre-stressing of connecting bolts. Parametric studies are conducted to show the non-linear effect of the rigidity, compared with a variation of bolt tightness. Additionally, the stress distribution is found, not only in the flange itself, but also in the bolts. It is interesting to note that under the tension of the connection, the bolts are subjected to bending. Next, a damaged connection with a broken or loose bolt is considered.

In the last part of the paper, the behaviour of the complex structure, composed of tubular beams and bolted connections, is investigated. The discussion includes the influence of a damaged connection on the tower deflection. The problem is solved by applying a multilevel substructuring approach, and a reduction of DOFs using static condensation method.

2. The structure under consideration

The paper deals with a telecommunication tower, composed of four truss/frame segments (Fig. 1), together assembled with CFBC. The tower is of a triangular cross section. It is composed of tubular, longitudinal members and tubular bracings. All of them constitute a truss like structure. However, on the contrary to the pin joints assumed in the truss design, here the connections joining longitudinal elements are considered to be elastic. They are composed of circular flanges and pre-stressed bolts (Fig. 2).

Due to a very large number of degrees of freedom in FEM analysis, a two level of substructuring to the whole tower is applied. The substructuring of the connection consists on dividing it in components, which are modelled separately, and then combined together. The substructuring of the tower consists on separate analyses of tower sections and connections, and then joining all of them in one structural system.

First of all, in Section 3, the non-linear FEM analysis of the connection is considered. As the result, CFBC rigidity, in the form of force–deformation relation is obtained. Additionally, results of the analysis show the bolt bending due to the prying effect.

An extended FEM analysis allows, moreover observing the behaviour of the connection with one or more bolts failed.

At the end of general consideration, the substrucuring and the condensation of tower segments and connections is discussed. This gives practical formulae allowing to find the response of the tower to external loads.

3. The dependence of the CFBC rigidity on bolt pre-tension

The discussed CFBC is presented in Fig. 2. It is composed of two similar flanges, each welded to a structural tube. The flanges are connected together with six bolts. The bolts, acting through washers, are pre-tensioned with prescribed forces. The material of flanges, bolts and pipes is steel, with Young modulus 205 GPa and Poisson ratio 0.3. The friction coefficient is assumed to be 0.5.

Owing to the non-linearity, the connection rigidity is understood as a ratio of the force variation Δf to the displacement variation Δu, between places where flanges are welded to the tubes. It means that tubes are not included in defining the connection rigidity. They are only needed for a proper modelling of place where the connection is linked to the tube.

The connection is modelled using 3D FEM in Abaqus/Standard (Fig. 3), with the finite-sliding, surface-to-surface contact formulations. The master and slave nodes are automatically assigned to surfaces by the program.

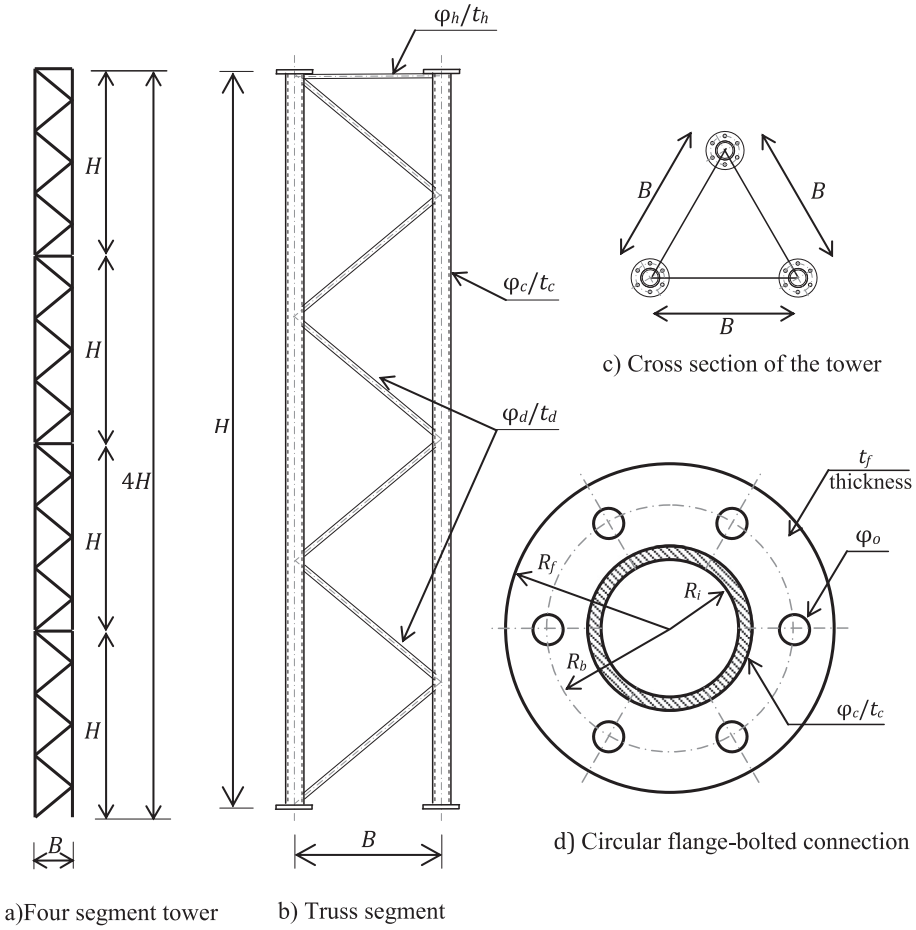

Fig. 1. Telecommunication tower and its components.

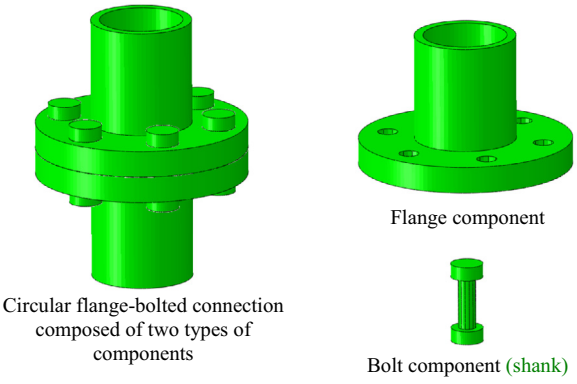

Fig. 2. Circular flange-bolted connection and its components.

The detailed model of CFBC is created using a *substructuring* technique [26]. According to the procedure presented by Rixen, the individual components of the CFBC are modelled separately, and then combined together, taking into account contact between them.

There are two different types of components for CFBC (Fig. 2). The first is the flange welded to a circular hollow section beam, and the second one is pre-tensioned bolt. The first component contains a 150 mm-long beam, which takes into account local interaction between flange and beam.

Two types of *isoparametric* continuum elements are applied. These are: quadratic tetrahedral C3D10 and quadratic hexahedral C3D20 elements, with 10 and 20 nodes per element, respectively.

The shape functions for the selected FE have the general form

$$N_i = N_i(\xi, \eta, \zeta), \quad i = 1, 2, \ldots, n^e_{DOFs}$$

The resulting stiffness matrix of an element consists of an elastic stiffness matrix and an initial stress stiffness matrix.

The elastic stiffness matrix, for assumed kinds of FE is as follows:

$$\mathbf{k}_e = \int_\Omega \mathbf{D}^T \mathbf{E} \mathbf{D} |\mathbf{J}| d\Omega \tag{1}$$

where **D** is a matrix containing derivatives of shape function, with respect to the coordinates related to the element (ξ, η, ζ), **E** is a matrix characterizing physical properties of the material, **J** is a Jacobian matrix of transformation from (ξ, η, ζ) to (x, y, z) coordinate system, and Ω denotes volume occupied by finite element.

The initial stress stiffness matrix has the following form

$$\mathbf{k}_\sigma = \int_\Omega \mathbf{G}^T \mathbf{S} \mathbf{G} |\mathbf{J}| d\Omega \tag{2}$$

where **G** is a matrix obtained from the differentiation of shape functions, and **S** is a matrix containing information about initial stresses within the element. Summing FE stiffness matrices, the stiffness matrices of both CFBC components are found and have the form

$$\mathbf{K}^{(f_i)} = = \left[\begin{array}{c|cc} \mathbf{K}_{II} & \mathbf{K}_{IC} & \mathbf{K}_{IB} \\ \hline \mathbf{K}_{CI} & \mathbf{K}_{CC} & \mathbf{K}_{CB} \\ \mathbf{K}_{BI} & \mathbf{K}_{BC} & \mathbf{K}_{BB} \end{array}\right]^{(f_i)} = \begin{bmatrix} \mathbf{K}_{ss} & \mathbf{K}_{sm} \\ \mathbf{K}_{ms} & \mathbf{K}_{mm} \end{bmatrix}^{(f_i)} \qquad i = 1, 2, \ldots, n_f \tag{3}$$

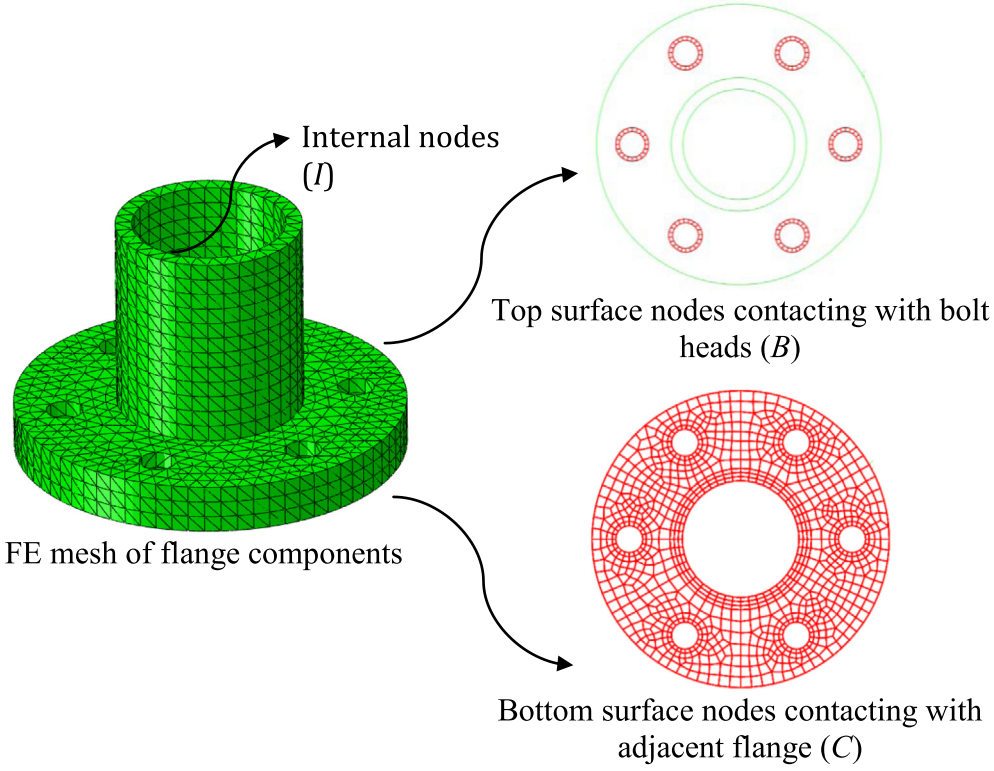

Fig. 3. Nodal partitions of flange components.

$$\mathbf{K}^{(b_j)} = = \left[\begin{array}{c|c|c} \mathbf{K}_{II} & \mathbf{K}_{IF_1} & \mathbf{K}_{IF_2} \\ \hline \mathbf{K}_{F_1 I} & \mathbf{K}_{F_1 F_1} & \mathbf{K}_{F_1 F_2} \\ \hline \mathbf{K}_{F_2 I} & \mathbf{K}_{F_2 F_1} & \mathbf{K}_{F_2 F_2} \end{array}\right]^{(b_j)} = \left[\begin{array}{cc} \mathbf{K}_{ss} & \mathbf{K}_{sm} \\ \mathbf{K}_{ms} & \mathbf{K}_{mm} \end{array}\right]^{(b_j)} \qquad j = 1, 2, \ldots, n_b \tag{4}$$

where F_1 – denotes bolt nodes, which are in contact with the upper flange component, F_2 – indicates contact nodes with lower flange component, and I is an index for internal nodes of bolt and flange components.

Having defined stiffness matrices for the both components, it is possible to model contact between them. To perform the contact model, the partition of component nodes for their individual groups (I, C, B) is done as presented in Fig. 3.

Combining all the components into one system, equilibrium equations for the total CFBC can be expressed in the following form:

$$\begin{cases} \mathbf{K}^{(c)}\mathbf{u}^{(c)} = \mathbf{f}^{(c)} + \mathbf{g}^{(c)}(\mathbf{u}^{(c)}) & \\ \mathbf{B}\mathbf{u}^{(c)} = \mathbf{0} & \text{-Compatibility condition} \\ \mathbf{L}^{\mathrm{T}}\mathbf{g}^{(c)}(\mathbf{u}^{(c)}) = \mathbf{0} & \text{-Equilibrium of contact (interface) forces} \end{cases} \tag{5}$$

where

$$\mathbf{K}^{(c)} = \begin{bmatrix} \mathbf{K}^{(f_1)} & \cdots & \mathbf{0} & \mathbf{0} & \cdots & \mathbf{0} \\ \vdots & \ddots & \vdots & \vdots & \cdots & \vdots \\ \mathbf{0} & \cdots & \mathbf{K}^{(f_{n_f})} & \mathbf{0} & \cdots & \mathbf{0} \\ \mathbf{0} & \cdots & \mathbf{0} & \mathbf{K}^{(b_1)} & \cdots & \mathbf{0} \\ \vdots & \cdots & \vdots & \vdots & \ddots & \vdots \\ \mathbf{0} & \cdots & \mathbf{0} & \mathbf{0} & \cdots & \mathbf{K}^{(b_{n_b})} \end{bmatrix}, \quad \mathbf{u}^{(c)} = \begin{bmatrix} \mathbf{u}^{(f_1)} \\ \vdots \\ \mathbf{u}^{(f_2)} \\ \mathbf{u}^{(b_1)} \\ \vdots \\ \mathbf{u}^{(b_{n_b})} \end{bmatrix} \tag{6}$$

Vector $\mathbf{f}^{(c)}$ contains all external forces applied to the connection, while $\mathbf{g}^{(c)}$ contains interface forces, including contact.

The simulation in finding rigidity is performed by applying Python, an object-oriented programming language, an interpreter of which is implemented in the Abaqus system. Owing to the non-linearity of the problem, the program finds the rigidity in an iterative way, using Newton's method.

Here, external axial forces f are applied to the ends of the flanges. Two different CFBCs are considered. The first one assumes 30 mm flange thickness, while in the second one, flange thickness equals 50 mm (Fig. 5). In both connections bolts M20 (shank of the bolt is used in calculations) are applied and both CFBCs connect the tubes of 114.3 mm diameter and wall thickness of 10 mm.

Axial loading is subjected through stresses, applied to cross-sections of tubes. The discussed force is then a product of stresses applied to the tube and its cross-section area. The FEM analysis is performed for the range of available stresses between the largest negative and the largest positive values of stresses of 200 MPa applied to the tubes. The analysis is done for four different values of pre-stressing bolt force; namely: 100; 80; 60; 40 kN. An example of the CFBC deformation is shown in Fig. 4.

The rigidities of the connections for different pre-stressing bolt forces are given in Fig. 7. For the compression, the diagram is linear and independent of bolt forces. In this case, the loading is transferred through direct contact between the flanges. This is not the case for tension. With the increasing load, the force–displacement diagram is partly non-linear, showing influences of the bolt and the contact forces.

It must be pointed out that deformation of a CFBC depends strongly on the geometric parameters of the flange and bolt pre-stressing. This can be seen clearly in Fig. 7 where two connections with different flange thicknesses are shown; both with unstressed bolts.

R_i	47.15 mm
R_b	90 mm
R_f	120 mm
t_f	30 mm
φ_o	22 mm
φ_c/t_c	114.3/10mm

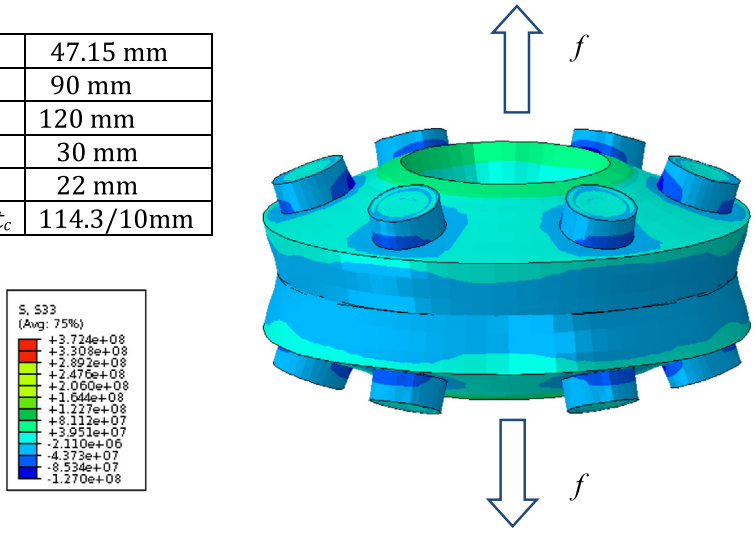

Fig. 4. The connection deformation under axial forces $f = 264$ kN, and pre-tensioned bolts to 60 kN.

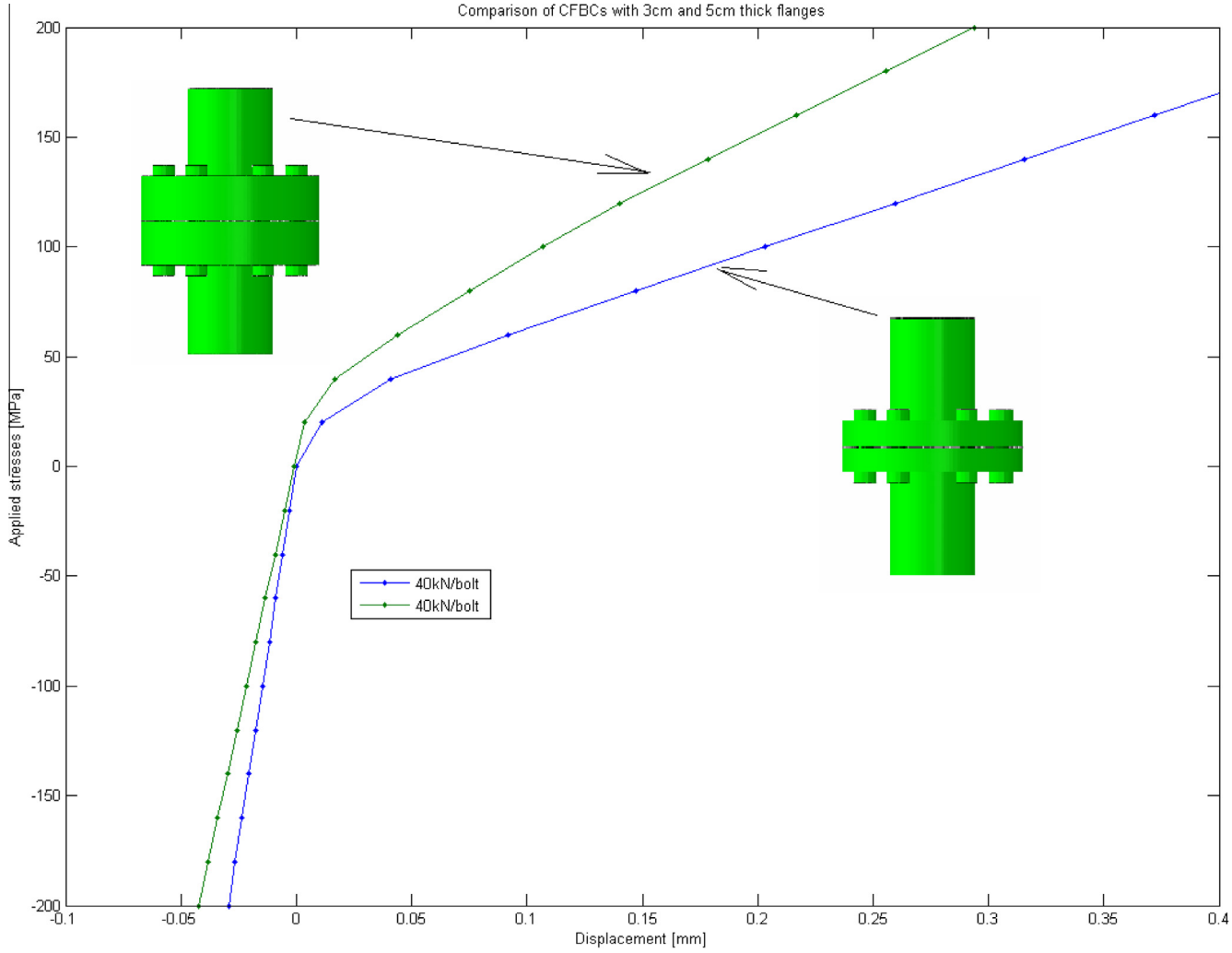

Fig. 5. Rigidity as force deformation relation for 30 mm and 50 mm flange thicknesses. Both with the same bolt diameters and pre-tensioning 40 kN/bolt.

4. Prying effect, bending and damage of bolts

Observing the stress picture of the cross-section of the pre-stressed connection (Fig. 9), it can be noted, that flanges are in contact, along outer borders. In the same time, due the flanges deformation, inner borders are separated. Such a state is known as a prying effect. It was already observed and discussed earlier, among others by Cao and Bell [6]. Below, Fig. 8 are two diagrams, the first

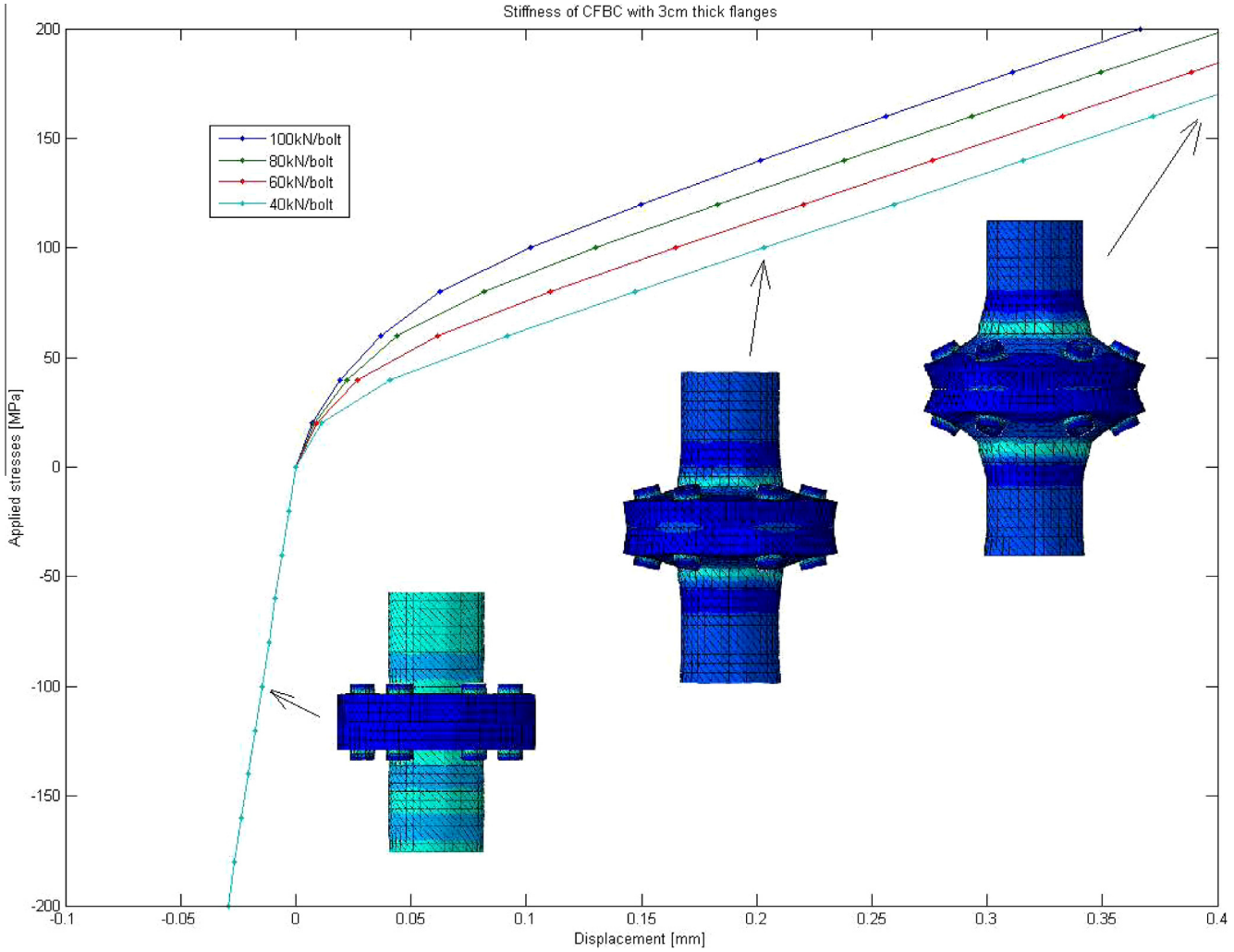

Fig. 6. Rigidity as force–deformation relation for 30 mm flange thickness, with the same bolt diameter and four different bolt pre-stressings.

one from Cao and Bell study, and the second one from numerical study in the present paper. Both represent relation between bolt forces and tension force applied to the connection. One may observe the same prying effect on both diagrams. Differences are in numbers, which come from different relations of flange thicknesses to their diameters. In connections discussed by Cao and Bell this relation is equal to 0.1 and in present paper equal to 0.25.

The flange deformations can take place without prying, as they depend on flange thicknesses and bolt pre-tensioning. With thicker flanges and smaller pre-tensioning, the prying effect disappears (Fig. 7b).

As a result of the flange deformation, heads of the same bolt rotate in opposite directions (Fig. 9). This causes bolt bending. This important fact should be taken into account in CFBC design, together with axial stresses, as the varying stresses in bolts, during tower vibration, might cause their fatigue collapse.

The maximal tension stresses in a bolt, as a function of the force applied to the connection through a tubular structural member, are shown in Table 1.

With the vibrations of the tower, the aforementioned stresses vary from σ_{press} to $\sigma_{\max}$ causing conditions for fatigue failure, or the loosening of one or more bolts. This would, of course, cause a decrease in connection rigidity, and in turn, cause larger deflections of the tower. In order to find numerical values for such a failure, let us return to the stiffness matrix $\mathbf{K}^{(c)}$ presented in the previous section. Removing from it the term related to one of bolts, a new matrix is found, which is applied for finding the damaged connection rigidity.

$$\mathbf{K}^{(c)} = \begin{bmatrix} \mathbf{K}^{(f_1)} & \dots & \mathbf{0} & \mathbf{0} & \dots & \mathbf{0} \\ \vdots & \ddots & \vdots & \vdots & \dots & \vdots \\ \mathbf{0} & \dots & \mathbf{K}^{(f_{n_f})} & \mathbf{0} & \dots & \mathbf{0} \\ \mathbf{0} & \dots & \mathbf{0} & \mathbf{K}^{(b_1)} & \dots & \mathbf{0} \\ \vdots & \dots & \vdots & \vdots & \ddots & \vdots \\ \mathbf{0} & \dots & \mathbf{0} & \mathbf{0} & \dots & \mathbf{K}^{(b_{n_b})} \end{bmatrix} \tag{7}$$

An example of a CFBC with two bolts damaged is presented in Fig. 10.

In Table 2, several combinations of flange thicknesses and number of removed bolts are presented. It might be worthy to note, that bending of bolts might have a significant influence on structural healthy. The bending effect depends clearly of flange thickness. The stresses due bending, are larger in the case of smaller thickness. In particular case the magnitude of stresses for flange thickness of 15 mm is above yield limit.

5. Decrease of connection rigidity, caused by a loose bolt, and its influence on displacements of the telecommunication tower

In this section, displacements of a telecommunication tower shown on Fig. 16 are considered. Two cases are discussed. The first

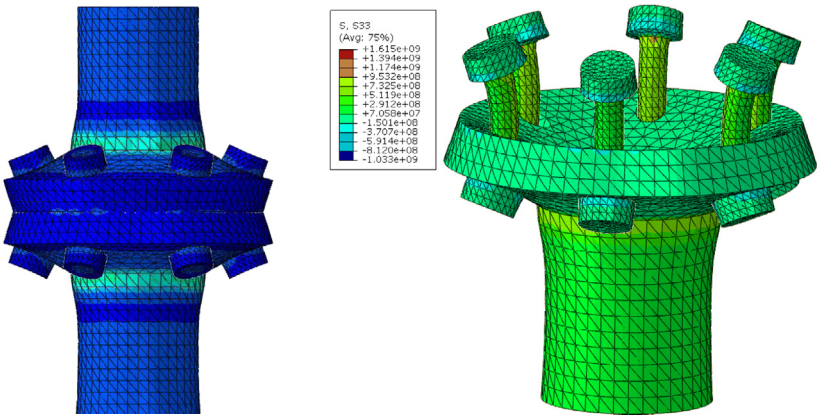

(a) Circular flange bolted joint with 30 mm thick flanges

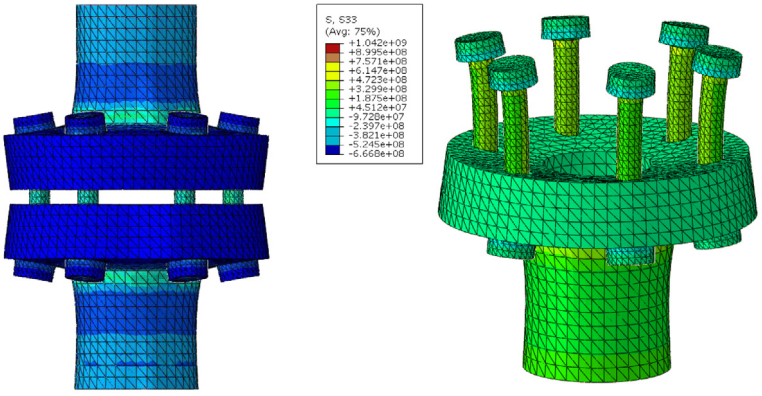

(b) Circular flange bolted joint with 50 mm thick flange

Fig. 7. Deformations of CFBC with two different flange thicknesses and non-pretensioned bolts.

one, when all connections are healthy, and the second one, when one of the connections is weakened by a loosen bolt.

The FEM model of CFBCs, discussed in Section 3, gives a rigorous view of the behaviour of the connection. However, in the case of composed structures, with larger numbers of structural members and connections joining them together, the model could be numerically too time-consuming. The problem is then solved by applying a multilevel substructuring approach, combined with static condensation, which allows for the reduction in the number of DOFs.

For the discussed tower, two levels of substructuring are considered. The first level contains basic elements of CFBCs, namely flanges and bolts. The results of substructuring for the connections are given in Section 3, using Eqs. (5) and (6).

In the second level, the substructuring of a truss segment is performed. Finally, the telecommunication tower is assembled joining all the truss and connection substructures. The idea of the proposed substructuring is presented in Fig. 11.

5.1. 1st level substructuring

Let us reduce the order of the presented model of CFBC, applying the static condensation approach. The static equilibrium Eq. (6) can be presented in the following form:

$$\mathbf{K}^{(c)}\mathbf{u}^{(c)} = \mathbf{f}^{(c)} + \mathbf{g}^{(c)}(\mathbf{u}^{(c)}) \tag{8}$$

Based on the results obtained from the detailed model, we can assume, before proceeding with condensation, that contact between bolt heads and top of flanges is never lost, and this brings us to the first observation: the bolt head is always in contact with flange. This assumption can be introduced by replacing the head of the bolt by a set of nodes, which is coupled with bolt deformation. Next, simplification is related to the fact that bolts exhibit only two main modes of deformation: mainly, extension and bending. Such behaviour can be implemented using beam elements with intermediate nodes (Fig. 12). Then, two end nodes are coupled with flange deformation, while the middle one is used to apply a pretensioning force. The cross-section of the beam is chosen as a circular profile, with the cross-section area corresponding to that of the bolt.

To reduce the number of degrees of freedom, the displacement vector $\mathbf{u}^{(c)}$ of the full model is now broken down into two parts. The first one, $\mathbf{u}_m^{(c)}$, is related to displacements of loaded nodes of the full model. The second one, $\mathbf{u}_s^{(c)}$ refers to unloaded joints. The subscripts m and s are referred to as master (kept) DOFs and slaves (deleted), respectively. With such assumptions, the static equation of CFBC can be partitioned as follows:

$$\begin{bmatrix} \mathbf{K}_{mm}^{(c)} & \mathbf{K}_{ms}^{(c)} \\ \mathbf{K}_{sm}^{(c)} & \mathbf{K}_{ss}^{(c)} \end{bmatrix} \begin{bmatrix} \mathbf{u}_m^{(c)} \\ \mathbf{u}_s^{(c)} \end{bmatrix} = \begin{bmatrix} \mathbf{f}_m^{(c)} + \mathbf{g}_m^{(c)}(\mathbf{u}_m^{(c)}) \\ \mathbf{f}_s^{(c)} \end{bmatrix} \tag{9}$$

Under the assumption that $\mathbf{f}_s^{(c)} = \mathbf{0}$, the solution of the above two equations gives the relation defining the master displacements.

$$\left(\mathbf{K}_{mm}^{(c)} - \mathbf{K}_{ms}^{(c)}\left(\mathbf{K}_{ss}^{(c)}\right)^{-1}\mathbf{K}_{sm}^{(c)}\right)\mathbf{u}_m^{(c)} = \mathbf{f}_m^{(c)} + \mathbf{g}_m^{(c)}\left(\mathbf{u}_m^{(c)}\right)$$

or

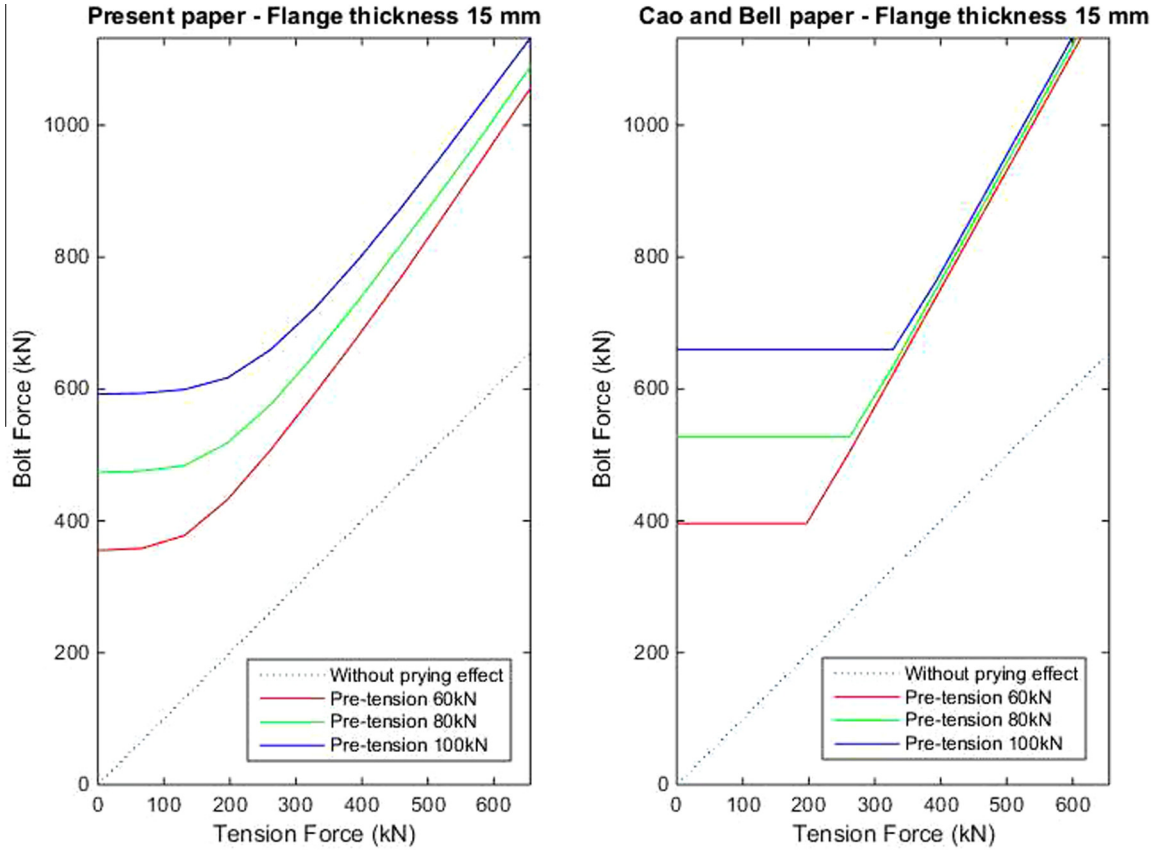

Fig. 8. Comparison of bolt force–tension force obtained in present paper and paper by Cao [6].

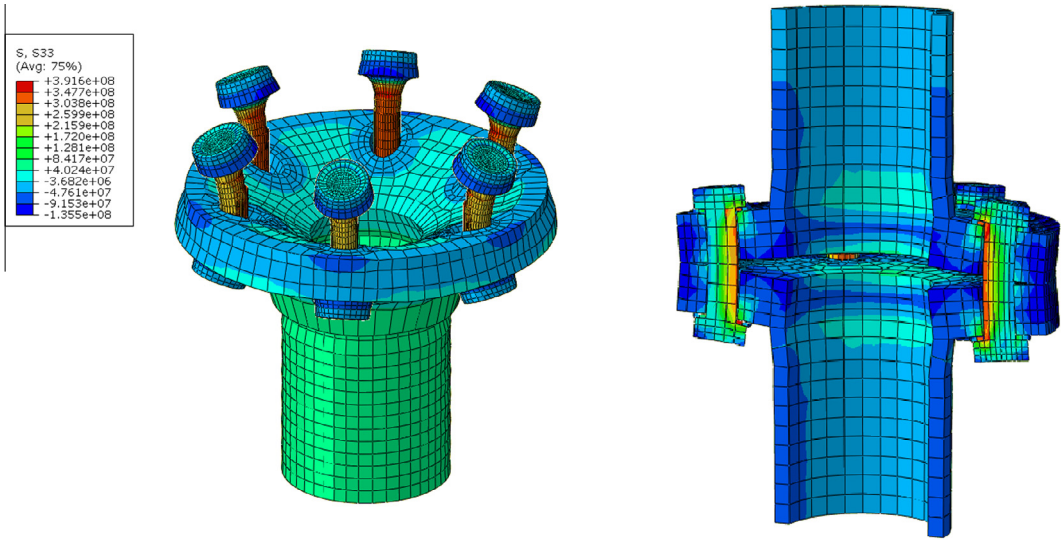

Fig. 9. Bending of bolts under tension of the connection.

Table 1
Stresses σ_{press} from pre-tensioning; maximal stresses σ_{max} equal to the sum stresses from tension and bending, under external tension equals 200 MPa.

Initial pre-tensioning force	40 kN	60 kN	80 kN	100 kN
σ_{press} (MPa)	127.3	190.9	254.7	318.3
σ_{max} (MPa)	602.5	613.8	625.1	636.5
$(\sigma_{max} - \sigma_{press})/\sigma_{press}$ (%)	373	221	145	99

$$\widetilde{\mathbf{K}}^{(c)}\tilde{\mathbf{u}}^{(c)} = \tilde{\mathbf{f}}^{(c)} + \tilde{\mathbf{g}}^{(c)}\left(\tilde{\mathbf{u}}^{(c)}\right) \tag{10}$$

where $\widetilde{\mathbf{K}}^{(c)}$ is the condensed stiffness matrix of the connection.

In the discussed case, external loads applied to master nodes are stresses at the cross-section of the tubes welded to the flanges, forces from pre-stressed bolts, and forces from truss elements. In particular, with regard to the connection discussed here, the number of 4928 nodes is reduced to 52. The latter are: 4 nodes

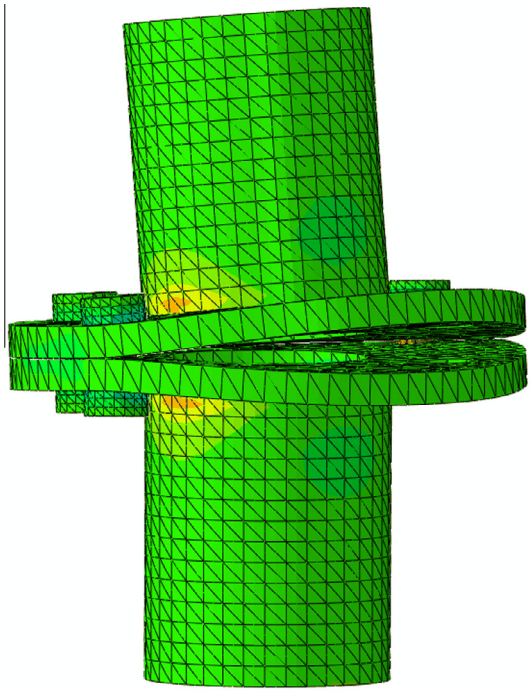

Fig. 10. Deformation of a connection with two damaged bolts, flange thickness 15 mm and four pre-tensioned bolts to 80 kN. The healthy connection given in Fig. 7.

Table 2
Max and min stresses (MPa) in 20 mm diameter bolts in all active bolts and in bolts next to the removed one. Yield limit for bolt class 8.8 is **640 MPa**.

	All bolts active		One bolt removed		Two bolts removed	
Flange thickness (mm)	15	50	15	50	15	50
σ_{min} (MPa)	136	363	627	371	−160	397
σ_{max} (MPa)	**1130**	471	**1700**	**658**	**2950**	**1130**

The values higher than 640 MPa are highlighted in bold.

connected to the column, bracings and horizontal pipes; 6 nodes are for connection with bolts; and 42 nodes as contact nodes between top and bottom flanges (Fig. 13).

The contact model applied here is partly simplified, compared to the one applied in Section 3. Here, the full model is replaced by a simpler contact model, containing elements called gap elements. They are defined in such a way that each pair of nodes potentially in contact is selected. In this way, an additional computational effort, required before to search for contact nodes, is significantly reduced. With these assumptions, the loads caused by contact and friction forces, are now denoted by $\tilde{\mathbf{g}}^{(c)}(\tilde{\mathbf{u}}^{(c)})$.

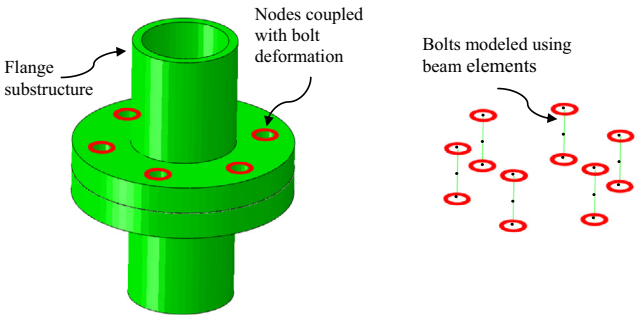

Fig. 12. Detailed CFBC model nodes coupled with those of reduced model.

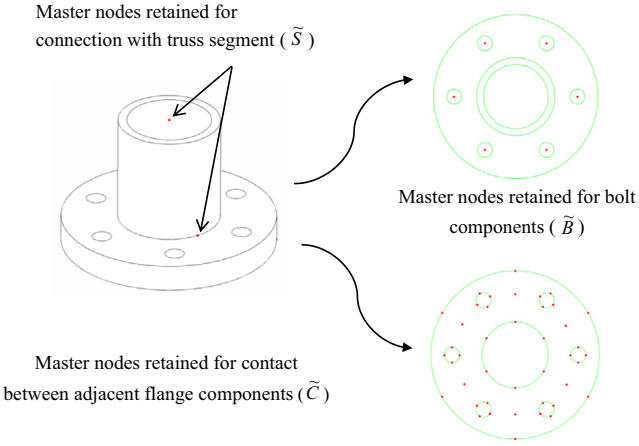

Fig. 13. Master nodes of reduced CFBC model.

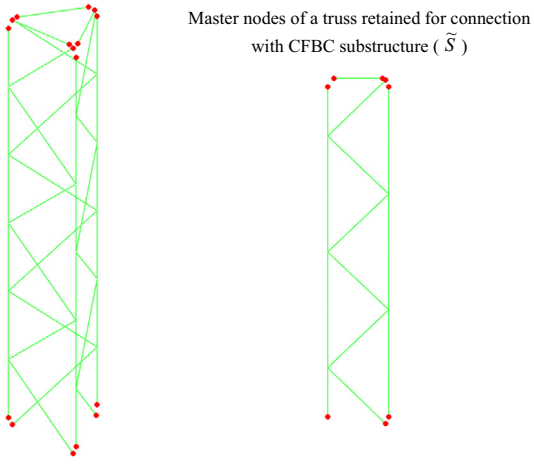

Fig. 14. A truss segment with nodes retained for connections with CFBCs.

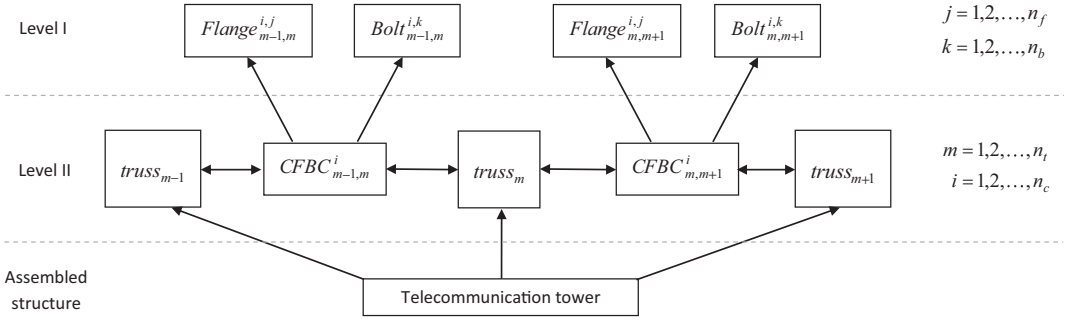

Fig. 11. Schematic representation of two-level substructuring for the telecommunication tower.

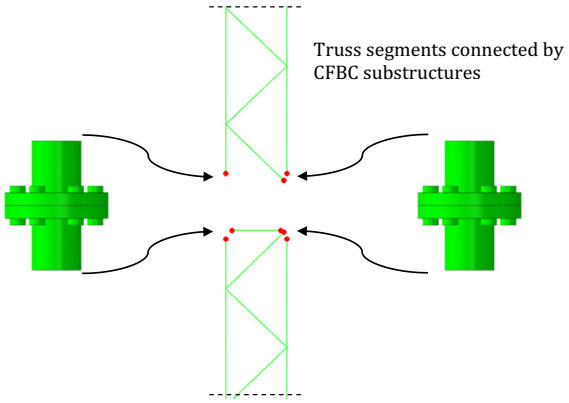

Fig. 15. Assembly of individual substructures into the telecommunication tower.

5.2. 2nd level substructuring

Let us now discuss substructuring and the condensation of a segment of the truss structure (see Fig. 14). The classical equation of equilibrium for the truss has the form:

$$\mathbf{K}^{(t)}\mathbf{u}^{(t)} = \mathbf{f}^{(t)} \tag{11}$$

Performing the same procedure for condensation, as in the case of the connection, the condensed stiffness matrix is obtained

$$\widetilde{\mathbf{K}}^{(t)} = \left(\mathbf{K}^{(t)}_{mm} - \mathbf{K}^{(t)}_{ms}\left(\mathbf{K}^{(t)}_{ss}\right)^{-1}\mathbf{K}^{(t)}_{sm}\right) \tag{12}$$

Subscripts denoting slave and master nodes are the same as for the connections.

Equilibrium equations for the tower, consisting of two types of substructures: connection and truss (Fig. 15), have the following form:

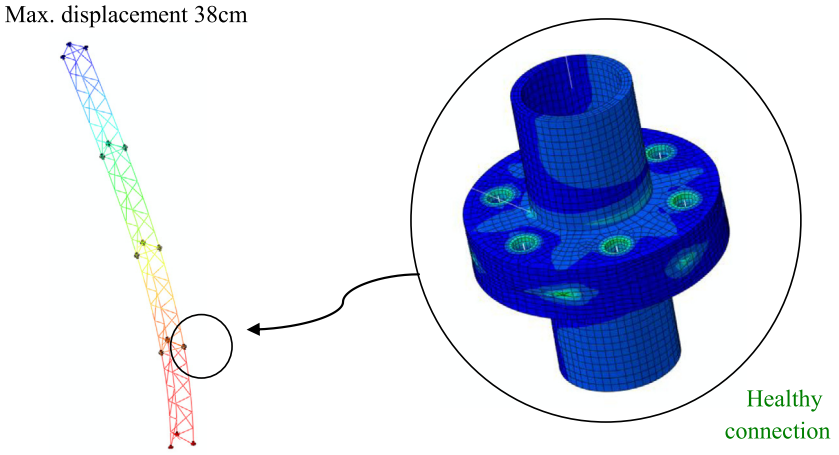

B	1.2 m
H	6.0 m
φ_h/t_h	48.3/3.2mm
φ_d/t_d	48.3/3.2mm
φ_c/t_c	76.1/3.2mm

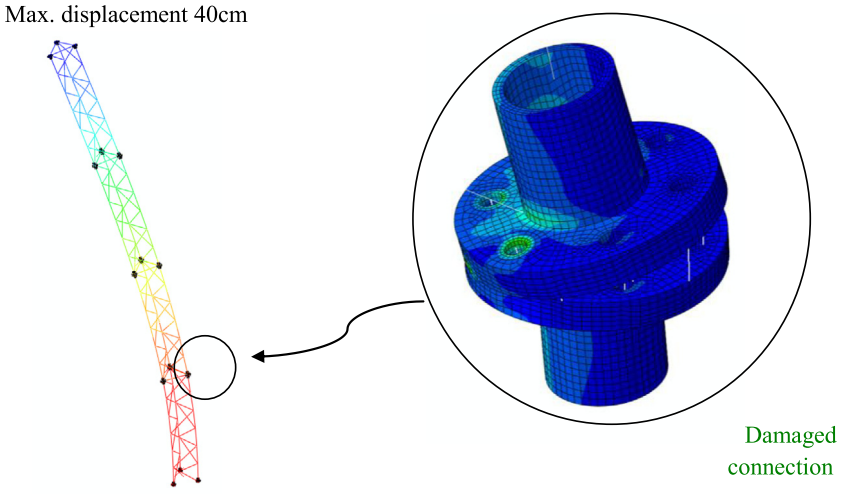

Fig. 16. Deflection of the telecommunication tower composed of four truss segments and joining them CFBCs.

$$\widetilde{\mathbf{K}}^{(T)}\tilde{\mathbf{u}}^{(T)} = \tilde{\mathbf{f}}^{(T)} + \tilde{\mathbf{g}}^{(T)}\left(\tilde{\mathbf{u}}^{(T)}\right)$$

where

$$\mathbf{K}^{(T)} = \sum_{i=1}^{n_t} \widetilde{\mathbf{K}}^{(t_i)} + \sum_{i=1}^{n_t-1}\sum_{j=1}^{n_c} \widetilde{\mathbf{K}}^{(c_{ij})}$$

and

$$\tilde{\mathbf{g}}^{(T)}(\tilde{\mathbf{u}}^{(T)}) = \sum_{i=1}^{n_t-1}\sum_{j=1}^{n_c} \mathbf{g}^{(c_{ij})}$$

In the above equations:

- n_t is number of truss segments in the tower,
- n_c is number of CFBCs connecting one truss segment with another,
- n_f is number of flange components constituting one CFBC,
- n_b is number of bolt components connecting one flange component with another.

6. Conclusions

A rigorous numerical analysis of CFBCs is presented. It includes contact and friction forces between flanges, between flanges and bolt washers. The analysis is performed by applying a substructuring approach. It means, a separate modelling of connection flanges and bolts, and then combining them together. To make the CFBC analysis more useful in practical design, the number of DOFs is reduced, by applying a static condensation approach.

It is observed that the non-linear rigidity of the connection depends not only on the sizes of elements, but also strongly upon the pre-tension forces in bolts (Fig. 6). It is worth noting that connection deformations depend significantly on flange dimensions (Figs. 5 and 7). Under tension, the stiffness increases with the increase of flange thicknesses, reducing in the same time prying effect (Fig. 8). Under compression, the connection with thicker flange thicknesses, deforms more than in the case of thinner flanges. This is because a thinner layer of a material deforms less than thicker one, under the same stresses.

It can be seen that the connection bolts are subjected to bending (Fig. 9), due the prying effect. The bending causes a significantly increase of stresses (Table 1), which should be taken into account in structural dynamics with fatigue effects.

Important information is obtained from the analysis of a CFBC with one and two loose bolts (damaged). The weakened rigidity of the connection is introduced into the design of a real tower, composed of four truss sections and twelve connections. The assembly of the tower is performed by applying two level substructuring and a reduction of DOFs by static condensation.

The differences in the deformations of two towers, one with all healthy CFBCs, and one with a damage connection, containing a failed bolt, are given in Fig. 16. They do not look very significant from the structural point of view. Nevertheless, in some cases, one removed bolt causes significant increase of the stresses in the neighbour bolts (Table 2).

References

[1] Heinisuo M, Perttola H, Ronni H. A step towards the 3D component method for modelling beam-to-column joints. Steel Constr 2014;7(1):8–13.
[2] Kim JH, Ghaboussi J, Elnashai AS. Hysteretic mechanical–informational modeling of bolted steel frame connections. Eng Struct 2012;45:1–11.
[3] Prinz GS, Nussbaumer A, Borges L, Khadka S. Experimental testing and simulation of bolted beam-column connections having thick extended endplates and multiple bolts per row. Eng Struct 2014;59:434–47.
[4] Málaga-Chuquitaype C, Elghazouli AY. Behaviour of combined channel/angle connections to tubular columns under monotonic and cyclic loading. Eng Struct 2010;32:1600–16.
[5] Schwingshackl CW, Di Maio D, Green JS. Modelling and validation of the nonlinear dynamic behaviour of bolted flange joints. In: ASME turbine technical conference and exposition, vol. 7A, structures and dynamics, 2013.
[6] Cao JJ, Bell AJ. Determination of bolt forces in a circular flange joint under tension force. Int J Press Vessels Pip 1996;68:63–71.
[7] Schaumann P, Seidel M. Failure analysis of bolted steel flanges. In: Proceedings of the 7th international symposium on structural failure and plasticity IMPLAST2000, Melbourne, Australia; 2000.
[8] Schaumann P, Kleineidam P. Global structural behaviour of ring flange joints. In: NAFEMS seminar: modelling of assemblies and joints for FE analyses, Wiesbaden, Germany; 2002.
[9] Pavlović M, Heistermann Ch, Veljković M, Daniel Pak D, Feldmann M, Rebelo C, Simões da Silva L. Friction connection vs. ring flange connection in steel towers for wind converters. Eng Struct 2015;98:151–62.
[10] Abidelah A, Bouchaïr A, Kerdal DE. Influence of the flexural rigidity of the bolt on the behavior of the *T*-stub steel connection. Eng Struct 2014;81:181–94.
[11] Gutkowski W, Blachowski B. Revised assumptions for monitoring and control of 3D lattice structures. In: 11th Pan-American congress of applied mechanics, Foz do Iguacu, Brazil, January 04–08, 2010.
[12] Swiercz A, Kolakowski P, Holnicki-Szulc J, Olkowicz D. Identification of semi-rigid joints in frame structures. In: 6th ECCOMAS thematic conference on smart structures and materials (SMART2013), Politecnico di Torino, 24–26 June 2013.
[13] Blachowski B, Swiercz A, Pnevmatikos N, Experimental verification of damage location techniques for frame structures assembled using bolted connections. In: COMPDYN 2015, 5th international conference on computational methods in structural dynamics and earthquake engineering, Greece; 2015.
[14] Bogacz R, Czyczuła W, Konowrocki R. Influence of sleepers shape and configuration on track-train dynamics, shock and vibration, 2014. p. 393867-1–7. [ISSN: 1070–9622].
[15] Stocki R, Tauzowski P, Knabel J. Reliability analysis of a crashed thin-walled s-rail accounting for random spot weld failures. Int J Crashworthiness 2008;13:693–706.
[16] Van-Long H, Jaspart JP, Demonceau JF. Behaviour of bolted flange joints in tubular structures under monotonic, repeated and fatigue loadings. I: Experimental tests. J Constr Steel Res 2013;85:1–11.
[17] Luan Y, Guan ZQ, Cheng GD, Liu S. A simplified nonlinear dynamic model for the analysis of pipe structures with bolted flange joints. J Sound Vib 2012;331:325–44.
[18] Couchaux M, Hjiaj M, Ryan I. Behaviour of bolted circular flange joints subjected to a bending moment and an axial force. In: 7th international workshop on connections in steel structures, Timisoara, 30 May–02 June 2012.
[19] Yang JN, Xia Y, Loh CH. Damage identification of bolt connections in a steel frame. J Struct Eng 2014;140(3).
[20] Pnevmatikos N. Damage detection of structures using discrete wavelet transform. In: Fifth world conference on structural control and monitoring (5WCSCM), Tokyo, Japan, 12–14 July 2010.
[21] He K, Zhu WD. Detection of damage in lightning masts and loosening of bolted connections in structures using changes in natural frequencies. In: Structural dynamics: vol. 3, Proceedings of the 28th IMAC, A conference on structural dynamics, Tom Proulx, 2010. p. 63–78.
[22] Perttola H, Heinisuo M. Experimental study on flanged joints of tubular members under biaxial bending. In: 7th international workshop on connections in steel structures, Timisoara, 30 May–02 June 2012.
[23] Henson GM, Hornish BA. An evaluation of common analysis methods for bolted joints in launch vehicles. In: 51st AIAA/ASME/ASCE/AHS/ASC structures, structural dynamics, and materials conference 18th, Orlando, Florida, 12–15 April 2010.
[24] Pitrakkos T, Tizani W. Experimental behaviour of a novel anchored blind-bolt in tension. Eng Struct 2013;49:905–19.
[25] An Y, Blachowski B, Ou J. A degree of dispersion-based damage localization method. Struct Control Health Monit 2016;23:176–92. http://dx.doi.org/10.1002/stc.1760.
[26] Rixen D. A dual Craig–Bampton method for dynamic substructuring. J Comput Appl Math 2004;168:383–91.